Solution of macroscopic state equations of blume-capel model using nonlinear dynamics concepts

Asaf Tolga ÜLGEN[1*], Naci SÜNEL[1]

[1]Department of Physics, Abant Izzet Baysal University, 14280 Bolu, Turkey e-mail:ulgen_at@ibu.edu.tr

19.09.2012 Geliş/Received, 06.11.2012 Kabul/Accepted

ABSTRACT

The macroscopic state equations of Blume-Capel Model were solved by using the concepts of nonlinear dynamics. Negative and positive exchange constant values yield bifurcations of pitchfork and subcritical flip types, respectively. Hence, we obtained bifurcations corresponding to second order phase transitions. The critical values of parameters were calculated from the neutral stability condition and the 3-dimensional phase diagram was plotted.

Key Words: BC Models, Phase Transitions, Bifurcation, Phase diagram

Blume-capel modelinin mikroskopik durum denklemlerini nonlinear dinamik kavramları kullanılarak çözümlenmesi

ÖZET

Blume-Capel Modelinin mikroskobik durum denklemleri nonlinear dinamik kavramları kullanılarak çözüldü. Negatif ve pozitif değiş-tokuş sabitlerinin değeri sırasıyla pitchfork ve subcritical dallanmalarını verir. Böylece dallanmaların ikinci dereceden faz geçişine karşılık geldiğini elde ettik. Parametrelerin kritik değerleri nötral kararlılık koşuluyla hesaplandı ve 3-boyutlu faz diyagramları çizildi.

Anahtar Kelimeler: Blume-Capel Model, Faz Geçişleri, Dallanmalar, Faz Diyagramı

1. INTRODUCTION

Different phases of magnetic materials are the macroscopic states corresponding to various reorganizations of micro-structures. Hence their investigation constitutes the cornerstone of the present technology. Moreover, transitions between different macroscopic states are important. In the early 1970s, successive phase transitions were observed experimentally in magnetic crystals [1, 2]. Blume-Capel (BC) Ising model has been mainly used to explain these transitions theoretically [3, 4]. In equilibrium statistics, the BC model has been solved by means of various methods, such as the mean-field approximation [3, 4], effective field theory [5], Bethe approximation [6], series expansion methods [7], renormalization-group theory [8], Monte Carlo simulations [9], the constant-coupling approximation [10] and cluster-variation method (CVM) [11].

BC model includes a bilinear Ising spin-1 model with exchange term and biquadratic terms with crystal field

* Sorumlu Yazar / Corresponding Author

constant. In the CVM, coupled nonlinear equations governing the order parameters which define the macroscopic states were obtained. In the literature, these equations have been solved by means of Newton-Raphson (NR) algorithm and the solutions give the magnetization and quadruple moments in the framework of equilibrium statistics [12, 13]. These quantities show different characteristic behaviors with temperature. Temperature dependence of magnetization gives rise to paramagnetic or ferromagnetic phases. At the phase transition temperature, the widespread NR algorithm cannot give a solution since the derivative of the function, which gives rise to nonlinearity in the equation governing the magnetization, vanishes. Therefore, plotting magnetization curves versus temperature has not been enough to find the phase transition temperature. In order to find this phase transition temperature, roots of Hessian determinant are calculated. Magnetization solutions which are found from NR algorithm do not give information whether they are stable or not. To get information about stability, free energy surface contours are plotted and from these plots, the stability of solutions are determined [14, 15]. This way of working is very cumbersome.

Macroscopic equations, which are found by BC model and its CVM, have been solved in the literature. Besides, non-linear dynamic concepts have been developed for 35 years. In this study, instead of NR algorithm, we solve macroscopic equations by means of mapping and these solutions are explained through non-linear dynamic concepts such as attractor, bifurcations 1-cycle and 2-cycle, neutral stable and super stable. Our method gives directed results without Hessian determinant and free energy surface contours.

2. THE MODEL AND ITS SOLUTIONS

2.1 The Model

The BC Ising model is defined by the following Hamiltonian

$$H = J \sum_{<ij>} s_i s_j + D \sum q_i \,,$$

where $s_i = 0, \pm 1$ at each lattice site, $< ij >$ indicates summation over all pairs of nearest-neighbor sites and $q_i = s_i^2$. J is the exchange constant and D denotes the single-ion crystal-field interaction. We have preferred to choose the Hamiltonian with plus sign, so $J < 0$ corresponds to ferromagnetic case and $J > 0$ corresponds to anti-ferromagnetic case and $J = 0$ corresponds to non-interacting spins, respectively.

According to the Ligand Field Theory (and Crystal Field Theory), the orientation of wave functions of the guest d-orbital in the ligand field causes an increase in the energy of guest electron when it is located in a place with high host electron density. Contrary to this, the orientation of wave functions of the guest d-orbital in the ligand field causes a decrease in its energy when it is located in a place with low host electron density [16]. This phenomenon is reflected by the second term in the above Hamiltonian. Electron paramagnetic resonance experiments show that $D < 0$ for $ZnO{:}\,Mn^{+2}$ and $D > 0$ for $CdSe{:}\,Mn^{+2}$ [17]. Numerical values of D depend on whether the ligand is octahedral, tetrahedral or cubic. As the radius of ligand becomes smaller and its negative charge becomes higher, D receives higher values. D can also be increased by increasing the charge of the metal (guest) atom and replacing metal atoms having 5dorbital instead of 3d-orbital[16]. In our calculations we considered $D \in$ (-3.0, +3.0)eV.

To the lowest order, the CVM gives us [12-15]

$$M = \frac{2\sinh(2\beta JM)}{e^{-\beta D} + 2\cosh(2\beta JM)} \equiv f(M) \qquad (1a)$$

and

$$Q = \frac{2\cosh(2\beta JM)}{e^{-\beta D} + 2\cosh(2\beta JM)} \,, \qquad (1b)$$

as the equations governing the magnetization and quadruple moment for spin-1 system. Here $\beta = 1/k_B T$ (k_B the Boltzmann constant), $M \equiv < s_i >$ and $Q \equiv < s_i^2 >$. Clearly, $-1 \le M \le 1$ and $0 \le Q \le 1$. External parameters are β^{-1}, J and D. All of these parameters are in the unit of eV.

Eq. (1a) has been solved by the NR algorithm which uses

$$M_i = M_{i-1} - \frac{F(M_{i-1})}{F'(M_{i-1})} \,,$$

where $F \equiv M - f(M)$ and F' is the derivative of F with respect to M. We have already mentioned the deficiency of this method in the introduction. Hence, in this work we shall follow another method that is introduced below [18].

2.2 Solution Technique

In this work, we use nonlinear dynamics; that is we consider iteration as a map. Eq. (1a) yields the map

$$M_{i+1} = f(M_i; \beta^{-1}, J, D) \qquad (1a')$$

and

$$M_{i+1} \equiv f(f(\dots f(M_0, \beta^{-1}, J, D) \dots))$$

$$i = 1, 2, 3, \dots, N$$

constitute the orbit initiating from the arbitrary value M_0 and belonging to the specified values of the control parameters of Eq. (1a′).

For given values of the control parameters, all orbits starting from arbitrary initial values may tend a certain point. This point is called a fixed point, M^*or 1-cycle. Some typical examples of 1-cycles are shown in Fig. 1. For other control parameter values, the same or some other fixed points might be obtained.

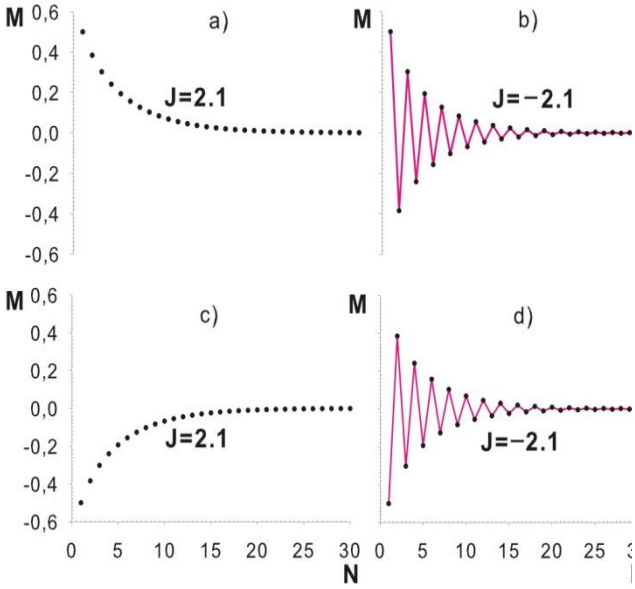

Figure 1. Orbit of the map given by Eq. (1a′). Parameter values are $\beta^{-1} = 0.25$ eV, $D = 2.2$ eV, $J = \pm 2.1$ eV. a) and b) for the initial value 0.5; c) and d) for initial value -0.5. The selected initial values are not important. Any initial value yields the same fixed point. Therefore the whole interval is the attraction domain of the fixed point zero.

If $|f'(M^*)| < 1, M^*$ is stable; if $|f'(M^*)| > 1, M^*$ is unstable; if $|f'(M^*)| = 0, M^*$ is super-stable and if $|f'(M^*)| = 1, M^*$ is neutral stable [18].

In the BC model, for Eq. (1a)

$$\frac{df(M)}{dM} = \frac{4\beta J \cosh(2\beta JM)}{2\cosh(2\beta JM) + \exp(-\beta D)} - \frac{8\beta J \sinh^2(2\beta JM)}{(2\cosh(2\beta JM) + \exp(-\beta D))^2} \quad (2)$$

is the function that will be used for the stability of fixed points. For some other values of the control parameters, a 2-cycle may be obtained. This means that two points alternatively appear: M_1^*, M_2^*. Some typical examples of 2-cycles are shown in Fig. 2. These 2-cycles are obtained from Eq. (1a′) for $J < 0$. However, when we consider $J > 0$ with the same β^{-1} and D, we get orbits of different character. This time, we have 2 fixed points having different sub-domains, [-1, 0) and (0, +1]. These orbits are shown in Fig.3. Stable fixed points and 2-cycles represent the macroscopic states that are the solutions of the dynamical equations so they determine magnetization and the quadrupole moment.

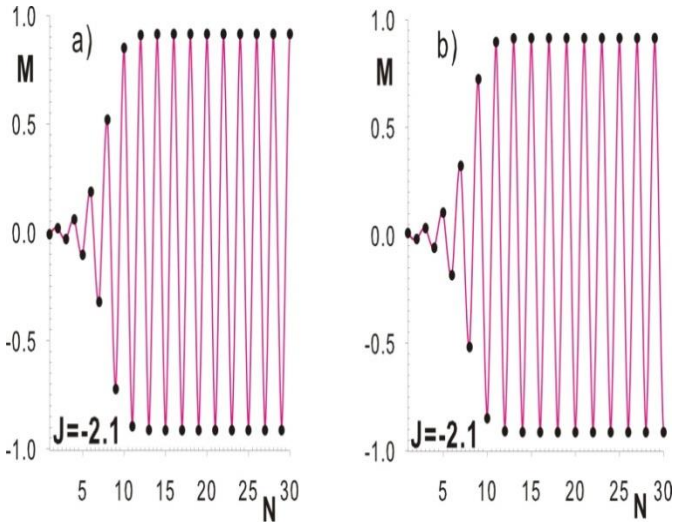

Figure 2. Orbit of the map given by Eq. (1a′): a) initiating from +0.001and b) initiating from -0.001. Values of the parameters are $\beta^{-1} = 0.5$ eV, $D = 2.2$ eV, J = -2.1 eV. The selected initial values are not important. Now the orbits yield a 2-cycle and the whole interval is the attraction domain of the 2-cycle.

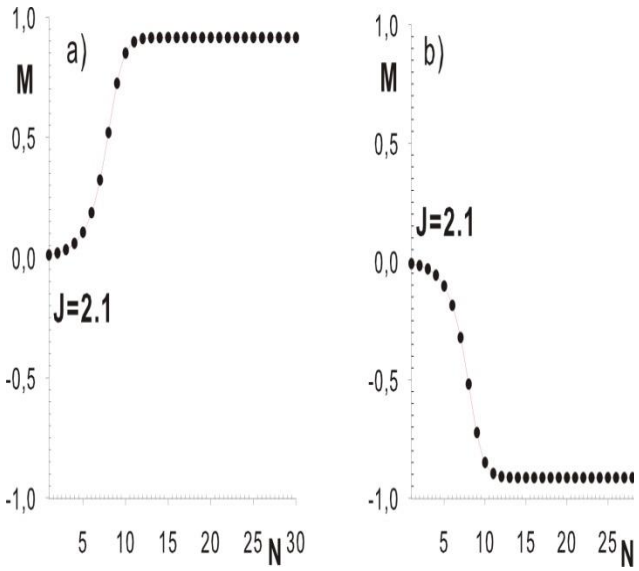

Figure 3. Orbit of the map given by Eq. (1a′): a) initiating from +0.001 and b) initiating from -0.001. Parameters values are $\beta^{-1} = 0.5$ eV, $D = 2.2$ eV, $J = +2.1$ eV. Orbits initiating from any point in the interval (-1, 0) yield the fixed point -1. Orbits initiating from any point in the interval $(0, +1)$ yield the fixed point $+1$. Since attraction domains of the fixed points ± 1 are different, these points do not form a 2-cycle.

Bifurcation, that is change of behavior of the physical system governed by the map, may occur when at least one of the control parameters cross the critical value. The notation β_c^{-1}, J_c and D_c will be used to denote the critical values. Bifurcation from 1-cycle to 2-cycle happens when a fixed point becomes neutral stable, *i.e.* $|f'(M^*)| = 1$. As we remember, Figs. 1, 2 and 3 depict the fixed points and two- cycles for a certain temperature value. By repeating the same procedure for each temperature value of k_BT $(0.0 - 3.5)$eV, we found all the fixed points and two-cycles belonging to each value of k_BT. Fig. 4 is obtained by plotting the fixed points and two-cycles versus k_BT. Thus, Fig. 4 is depicting the bifurcation diagrams of magnetization and macroscopic quadruple moment when *J* and *D* are kept constant. These are the diagrams showing the whole behavior of the physical system and also the values of the control parameter at which the system changes its behavior, *i.e.*, phase transitions. Stable fixed points (black circles) represent the states that the system prefers.

On the other hand, the unstable fixed points (dots) correspond to the states that the system does not prefer. When all of the spins are up, the magnetization of the system is1. In the opposite case, the magnetization is -1. When some of the spins are up and the rest are down, the magnetization takes any value between 1 and -1. $M^* = 0$ is a trivial solution for all parameter values. However, the interesting point is that it is a stable solution only in the A and C phases. At the bifurcation points the system

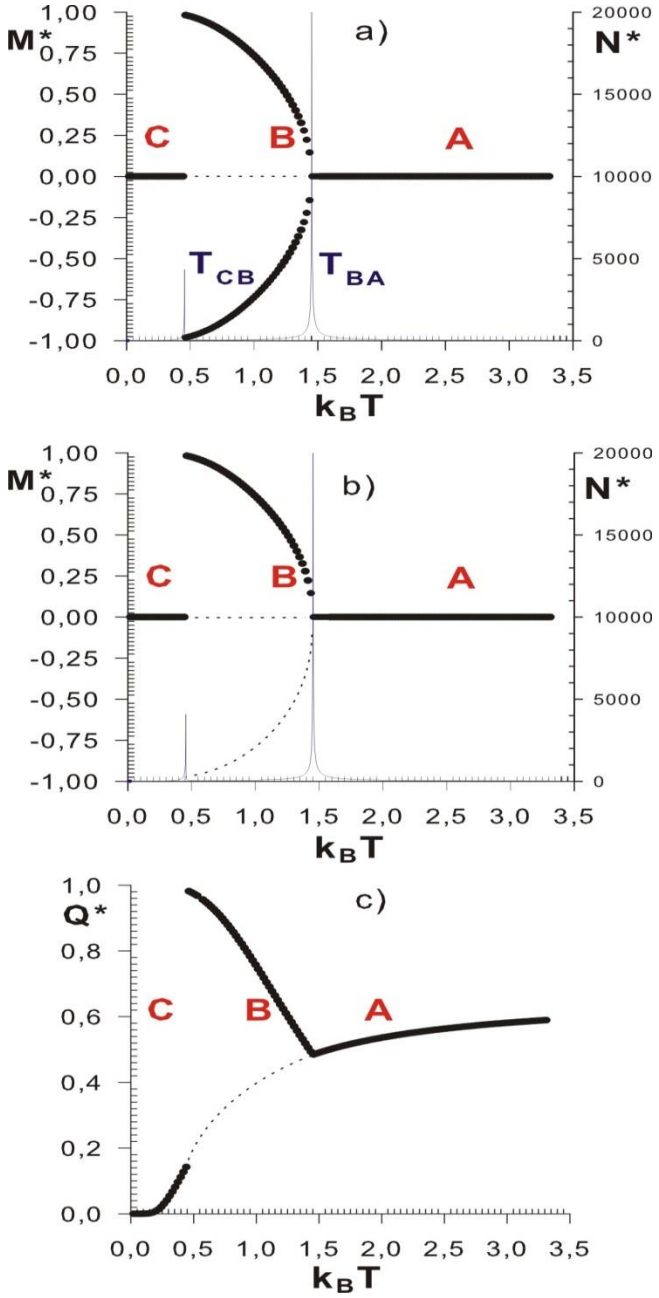

loses its behavior and reorganizes itself to attain a new behavior.

Another sign of stability of a fixed point is the cycle numberN^*. This number, as seen from Figs. 1 and 2, is the number of iteration until the fixed point is reached. In the A and C phases the stable fixed points are reached after 10 to 300 cycles; whereas at the bifurcation points the cycle number N^* reaches enormous values, such as at C-B transition $N^* \approx 5000$, and B-A transition $N^* \gg 20\,000$.

In Fig. 4, the unstable solutions are depicted by dotted curves. At the C-B phase transition, the system quits the

previous equilibrium and reorganizes itself. If $J < 0$, at a certain temperature, Eq. (1a′) accepts a 2-cycle solution. Thus, a $0 < M^* < 1$ stable solution and a $-1 < M^* < 0$ stable solution of Eq. (1a′) arise for each temperature value in a certain interval. These solutions exist in the β^{-1} (ork_BT) range ($0.5 - 1.5$eV). While β^{-1} decreases M^* values increase. In Fig. 4a, we mark the increasing M^* values. At the first glance, one may fall a misunderstanding by thinking that the system takes 2 different magnetization at a temperature. This is not so. The system can prefer one of these two stable solutions. What we want to show with this figure is only the temperature dependence of system's magnetization. The solution preferred by the system depends on the fluctuations of the control parameters and the initial conditions. If $J > 0$, Eq. (1a′) does not accept a 2-cycle stable solutions but 1-cycle (fixed point) stable solutions (Fig. 3). Therefore in Fig. 4b in the B phase we have only one curve showing again the β^{-1}dependence of 1-cycles. Dotted curves in Figs. 4a and 4b represent the unstable solutions.

Figure 4. Bifurcation diagrams for M^* and Q^*. a) for J = -1.5, D = -1.1; b) for $J = 1.5, D$ = -1.1 in eV units. Bifurcation occurs at 1:4518 eV. The stable $M_i^*, i = 1, 2$ curves are shown. The unstable solution is the dotted curve. Vertical axis on the left side of the graphs a) and b) represents magnetization (M^*), and the right side axis represents the iteration step numbers (N^*) up to fixed points. Q^* curve deviates from zero when β^{-1} approaches β_{CB}^{-1} from below.

At the bifurcation points, Eq. (2) takes the form

$$\left.\frac{df(M^*)}{dM}\right|_{M^*=0} = \frac{4\beta J}{2 + \exp(-\beta D)}\,, \qquad (3)$$

which yields the following relations between the control parameters: For stable M^*,

$$4\beta|J| < 2 + \exp(-\beta D)\,; \qquad (4a)$$

for unstable M^*(beginning of bifurcation),

$$4\beta|J| > 2 + \exp(-\beta D)\,; \qquad (4b)$$

for super stable M^*,

$$4\beta|J| = 0 \qquad (4c)$$

and for neutral stable M^*,

$$4\beta|J| = 2 + \exp(-\beta D)\,. \qquad (4d)$$

Condition (4c) is satisfied for either $\beta = 0$, *i.e.* at the high temperature limit, the system is super stable (M^*=0) or $J = 0$.

3. NUMERICAL RESULTS AND DISCUSSION

In the $J < 0$ case, as is seen from bifurcation diagram, the bifurcation at T_{BA} is of pitchfork type. The first term in the Hamiltonian is negative and the spins force each other to align. But in $J > 0$ case, the bifurcation at $T_{BA}$is subcritical flip [18], as is seen from Fig. 4b. This is the ferromagnetism (phase B in Figs. 4a and 4b).

As is well known, the tangent and pitchfork bifurcations are related to the second-order phase transitions [19]. Therefore the phase transition from phase A to phase B is of second order. But a first order phase transition includes discontinuity in magnetization. Therefore the B-C transition is of first order (Fig. 4). Hence, for $D < 0$, two successive phase transitions (firstly second order and secondly first order) appear while for $D > 0$ only a second order phase transition appears (Fig. 5). In our work, the phase transition temperatures are the values where the bifurcations occur. Hence, plotting magnetization versus temperature using Eq.(1a′) gives us precisely the phase transition temperatures. Moreover, Eq. (4d) provides us with a more direct way of finding the phase transition temperature without solving Eq.(1).

Fig. 4a gives evidence a pitchfork bifurcation in the magnetization curve at $\beta_{BA}^{-1} = k_BT_{BA}$. This is the phase transition temperature from the paramagnetic phase to the ferromagnetic phase. At $\beta_{CB}^{-1} = k_BT_{CB}$, the period doubling ends and we get zero fixed points. Therefore, we may conclude that at β_{CB}^{-1} a discontinuous bifurcation happens. In Fig. 4b, a subcritical flip bifurcation occurs just at T_{BA}. The phase transition corresponding the bifurcation at T_{BA} is a second order while the bifurcation at $T_{CB}$is of first order for both $J < 0$ and $J > 0$. As we have found the temperature variation of magnetization we easily deduce the temperature variation of Q^* by Eq. (1b). Q^* bifurcates also at the same critical temperatures.

In Figs. 4a and 4b, the temperature region named A, where the dipole moment vanishes but the quadruple moment takes a non-zero value, is interpreted as a representation of a disordered phase, the paramagnetic phase. The region named B, where both the dipole and quadruple moments are non-zero, clearly corresponds to an ordered ferromagnetic phase. Phase C appears only if $D < 0$. Because $M^* = 0$, phase C is a paramagnetic phase. However, this paramagnetic phase interpretation does not seem acceptable since in the near vicinity of absolute zero a complete disorder cannot be possible. At the crossing of paramagnetic and ferromagnetic regions, a second order phase transition is evident from Fig. 4a.

But if the phase C would represent a new magnetic organization other than paramagnetic one, the transition

at the crossing of ferromagnetic phase to phase C ought to be of second order. However, because of the discontinuity, the transition from B to C is of first order (Fig. 4a). On the other hand, as mentioned above, first order phase transition from B to C is a contradiction.

Q^* curve has two pieces in region C: Up to T_q it is zero and above T_q it shows a parabolic behavior (Fig. 4c). Hence below T_q the system is paramagnetic. However, we want to repeat here our remarks that were mentioned earlier: Above T_q, the phase is not paramagnetic because $M^* = 0$ but $Q^* \neq 0$. Fig. 5 shows the bifurcation diagrams versus D for various $\pm J$ values. With increasing D, the shift to higher values of the critical temperature belonging to second order phase transition is clear for both negative and positive J interactions. First order phase transitions occur for only negative values of D but disappear as $D \to 0$. Second order phase transitions always exist independently of J, even for $D = 0$.

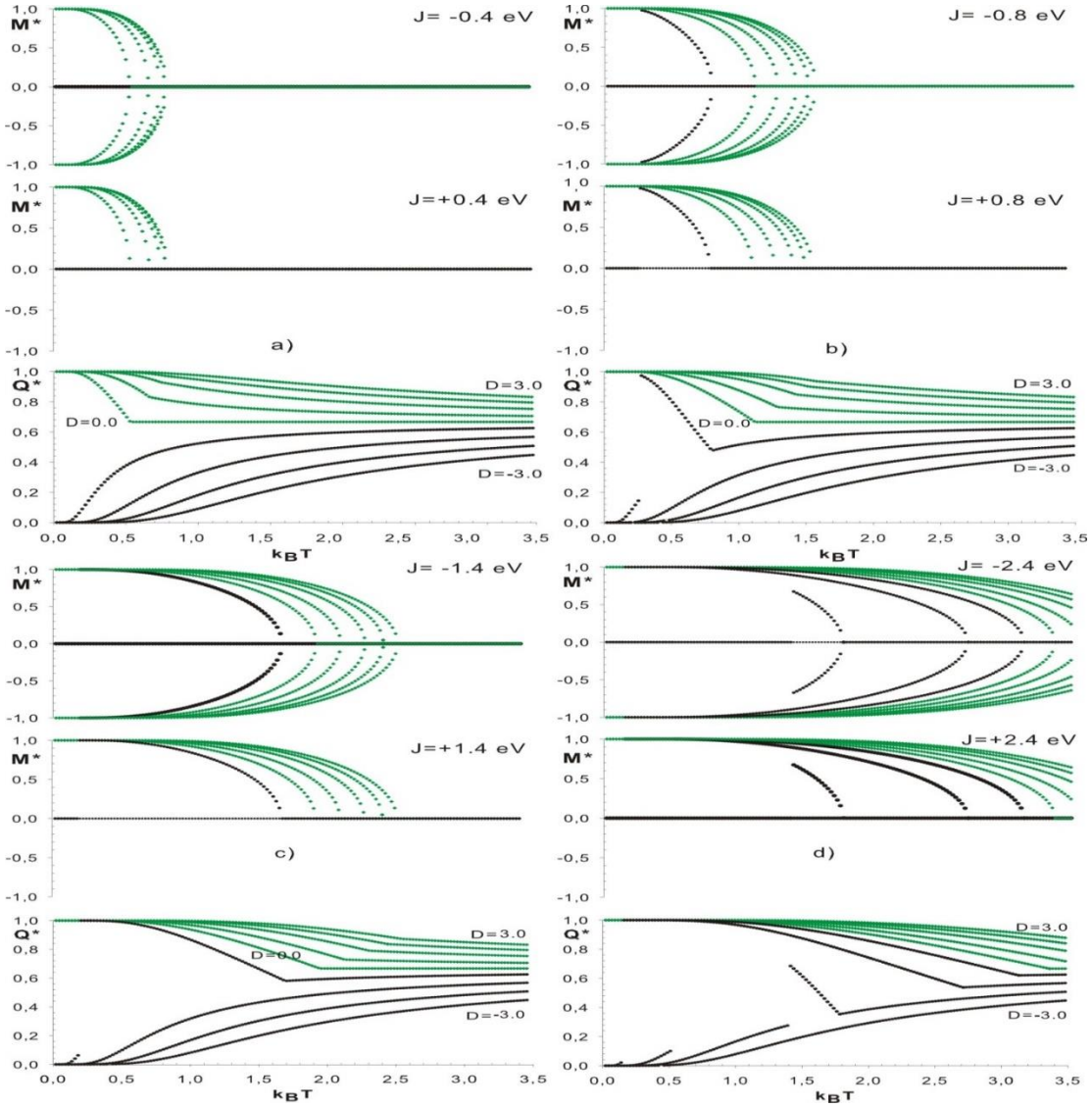

Figure 5. Critical temperature shift as the crystal field increases. a) $J = \pm 0.4$, b) $J = \pm 0.8$, c) $J = \pm 1.4$ and d) $J = \pm 2.4$ eV. Each graph consists of curves belonging to $D = 0.0, \pm 0.6, \pm 1.4, \pm 2.2$ and $\pm$ 3.0 eV.

When the critical temperature is used instead of phase transition β value, Eq. (4d) can be rewritten as

$$k_B T_C = \frac{4|J|}{2 + e^{-D/k_B T_C}} \quad . \qquad (5)$$

We solve Eq. (5) using the graphical technique, that is we plot the curves defined by both sides on the same axes system and find the intersection points (Fig. 6).

Fig. 6 shows that for $D > 0$, the second order phase transition temperature increases with increasing D. But for $D < 0$ the first order phase transition temperature reduces and the second order phase transition temperature increases as $D \to 0$. For $D > 0$, the first order phase transition disappears. Besides, for $D = 0$, a second order phase transition appears. This last finding is also supported by the magnetization curve plots in Fig. 5. On the other hand, when $D = 0$ the Hamiltonian consists only the Ising term. For spin 1, according to our investigation, a second order phase transition theoretically exists (Fig. 5), *i.e.* spontaneous magnetization can be observable.

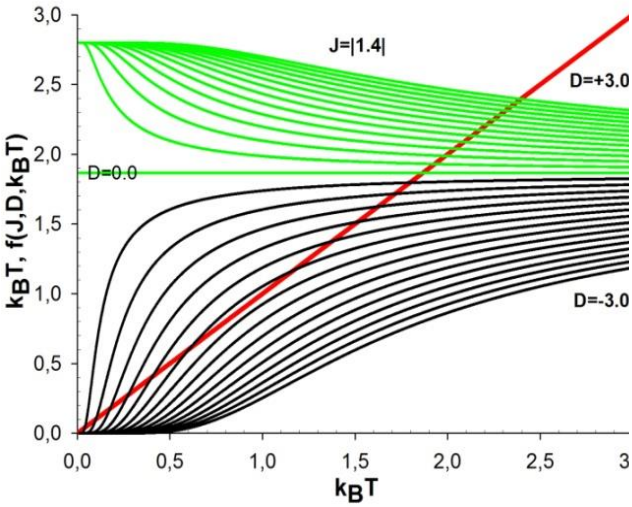

Figure 6. Graphical solution of Eq. (5) for $J = |1.4|$ eV. For $D > 0$ we have only one intersection point determining the second order phase transition temperature; for $D < 0$ we have either two or zero intersection points depending on D values. In the first case, the first intersection point determines the first order phase transition and the second intersection point determines the second order phase transition temperatures, respectively.

In Fig. 7 we show the phase diagrams obtained by using the numerical results derived from Fig. 6. In the literature, the phase diagram is generally plotted in two dimensions by defining the axes as D/J and k_BT/J, the reduced parameters. In these phenomena, the sign of D and J play a role. By using D/J axis, we lost the signs of D and J, *e.g.* D/J becomes positive for both $+/+$ and $-/-$ whereas D/J becomes negative for both $+/-$ and $-/+$. For this reason, information is partly lost. To overcome this difficulty, we preferred to plot the phase diagram in 3-dimensions. Our axes are k_BT, J and D.

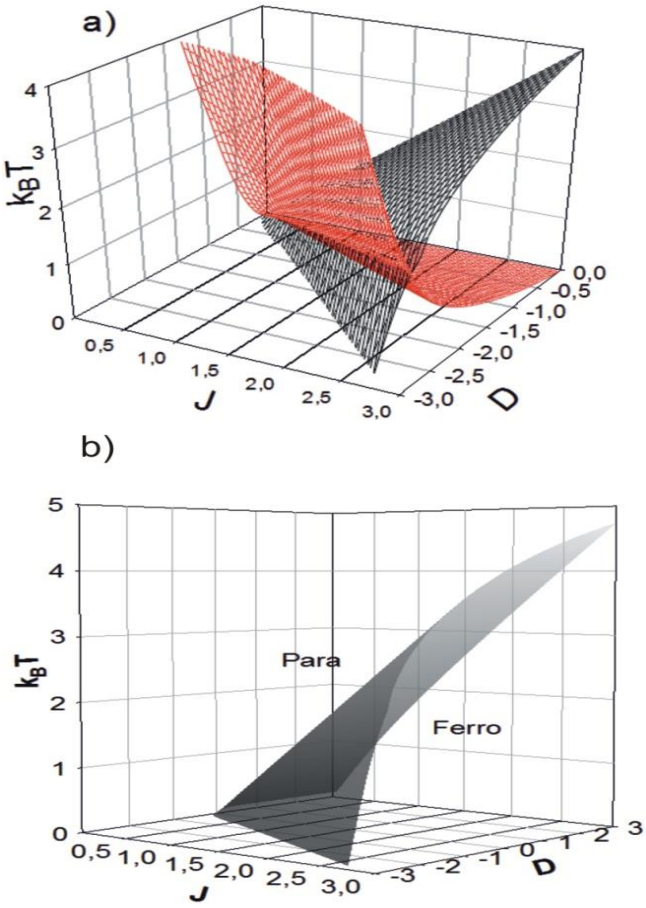

Figure 7. Phase diagram obtained for the B-C model with spin 1. a) $J \in (0.0, 3.0)$eV, D $\in (-3.0, 0.0)$eV and $\beta \in (0.0, 3.5)$eV. Red surface (C-B transition) is the surface on which first order phase transition occurs. Black surface (B-A transition) is the surface on which second order phase transition occurs. b) $J \in (0.0, 3.0)$eV, D $\in (-3.0, 3.0)$eV and $\beta \in (0.0, 3.5)$eV.

In calculations done with reduced quantities, Boltzmann constant is considered to be 1. One can approach to absolute zero of temperature without considering the investigated material. But in experiments, what is reduced to absolute zero is temperature itself. The important problem is to observe materials having interesting magnetic behavior near absolute zero [20, 21]. Therefore we preferred using temperature instead of reduced temperature.

In our numerical calculations due to the hyperbolic functions in Eq. (1), we could not approach to absolute zero and truncated at 40 K although double precision was used (Real*8) in our fortran code. If the value of temperature is taken below 40 K, an overflow error

occurs. The temperature limit decreased to 32 K when Real*16 precision was used. This temperature limit is due to the numerical calculation of exponential terms.
From Figs. 4 and 5, we see that the phase transition points remain the same under the $J \rightarrow -J$ transformation. Using this symmetry, we have plotted the phase diagram only for $J > 0$. Fig. 7a is depicting the phase diagram only for the negative D values. Concave upward surface represents the first order phase transition where the concave downward surface represents the second order phase transition.

The left side domain of the concave downward surface corresponds to paramagnetic state while the right side domain corresponds to the ferromagnetic state. The concave upward surface separates both the paramagnetic and ferromagnetic domains. In the literature, these lower parts are called as dense and the upper parts are named as diluted paramagnetic/ferromagnetic domains [12,13]. The intersection curve of the concave upward surface with the concave downward surface corresponds the embryo of ferromagnetic phases. In 2-dimensions, this curve is replaced by a certain point, called tricritical point. For all values of D second order phase transitions are observed.

4. CONCLUSION

In this work, we propose to use the concepts of nonlinear dynamics to calculate phase transitions in the spin-1 BC model. Phase transition temperatures are related to the bifurcation points. Second order phase transitions correspond to pitchfork and subcritical flip bifurcations. Moreover we obtained a simple equation from which we directly find the phase transitions without using the Hessian and free energy surfaces. Our method directly gives both second and first order phase transitions. In the literature, the second order phase transition can be calculated from Eq.(1a) but the first order phase transition is only obtained from free energy surface contours. The thermodynamical phenomena is invariant under $J \rightarrow -J$. Even for $D = 0$ case, a second order phase transition has been observed at finite temperatures. The phase C in Figs. 4 and 5 appears for only negative D values. In this phase, both $M^* = 0$ and $Q^* \rightarrow 0$. When both are zero, the phase is completely disordered. Here we believe that there are three open questions: (a) Transition from phase B to phase A is of second order. If phase C is paramagnetic just like phase A, why must phase C-B transition not be second order? But our calculations give a first order magnetic phase transition. (b) Can paramagnetic phase exist near vicinity of absolute zero? (c) During the numerical solution of Eqs. (1a) and (4d) at temperatures below 32 K we obtained an overflow. What is the behavior below this temperature? In future we hope that these questions will be figured out at least partially.

ACKNOWLEDGMENTS

With great appreciation, we thank Dr. E. Rızaoğlu for correcting the manuscript.

REFERENCES

[1] Cooke A H, Martin D and Wells M R, Solid State Commun **9**, 519 (1971).

[2] Sayetat F, Boucherle J X, Belakhovsky M, Kallel A, Tcheou F and Fuess H, Phys. Letters **35A**, 361 (1971).

[3] Capel H W, Physica **32,** 966 (1966).

[4] Blume M, Phys. Rev. **141**, 517 (1966).

[5] Siqueira A E, Fittipaldi I P, Physica A **138**, 599 (1986).

[6] Tanaka Y, Uryˆu N, J. Phys. Soc. Japan **50**, 1140 (1981).

[7] Saul D M, Wortis M, Stauffer D, Phys. Rev. B **9**, 4964 (1974).

[8] Berker A N, Wortis M, Phys. Rev. B **14**, 4946 (1976).

[9] Arora B L, Landau D P, Proc. AIP **5**, 352 (1972).

[10]Takanaka M, Takahashi K, Phys. Stat. Sol. B **93**, K85 (1979).

[11]Ng W M, Barry J H, Phys Rev B **17**, 3675 (1978).

[12]Ekiz C, Keskin M, Yalçın O, Physica A **293**, 215 (2001).

[13]Keskin M, Ekiz C, Yalçın O, Physica A **267**, 392 (1999).

[14]Keskin M, Özgan Ş, Physica Scriptia **42**, 349 (1990).

[15]Özsoy O, Keskin M, Physica A **319**, 404 (2003).

[16]Cotton F A, *The Crystal Field Theory. Chemical Applications of Group Theory, 3nd ed.* (John Wiley& Sons, New York, 1990).

[17]Kuang X Y, Phys. Lett. A **213**, 89 (1996).

[18]Thompson J M T, Stewart H B, *Nonlinear Dynamics and Chaos, 2nd ed.* (John Wiley& Sons, 2002).

[19]Schuster H G, Just W, *Deterministic Chaos*, (Wiley-VCH Verlag, Weinheim, 2005).

[20]Wigger G A, Felder E, Monnier R, and Ott H R, Pham L, Fisk Z, Phys. Rev. B, 014419 (2005).

[21]Rößler S, Harikrishnan, Naveen Kumar C M, Bhat H L, Elizabeth Suja, Rößler U K, Steglich F, Wirth S, J Supercond Nov Magn **22**, 205-208 (2009).